

# Pumping $K\alpha$ Resonance Fluorescence by Monochromatic X-Ray Sources

Sultana N. Nahar<sup>1,\*</sup> and Anil K. Pradhan<sup>1,2,3,†</sup>

<sup>1</sup>Department of Astronomy,<sup>2</sup> Chemical Physics Program,

<sup>3</sup> Biophysics Graduate Program, The Ohio State University, Columbus, Ohio 43210.

We demonstrate the correspondence between theoretically calculated K-shell resonances lying below the K-edge in multiple ionization states of an element [1], and recently observed  $K\alpha$  resonances in high-intensity X-ray free-electron laser (XFEL) plasmas [2]. Resonant absorptions in aluminum ions are computed and found to reproduce experimentally observed features. Results are also presented for titanium for possible observation of  $K\alpha$  resonances in the 4.5-5.0 keV energy range. A possibly sustainable excitation mechanism for  $K\alpha$  resonance fluorescence might be implemented using two monochromatic X-ray beams tuned to the K-edge and the  $K\alpha$  resonant energies simultaneously. This targeted ionization/excitation would create inner-shell vacancies via Auger decay, as well as pump  $K\alpha$  resonances. The required X-ray fluence to achieve resonance fluorescence would evidently be much less than in the XFEL experiments, and might enable novel biomedical applications.

**PACS number(s)** : 32.80.Aa, 32.80.Hd, 61.80.Cb, 87.53.-j, 61.80.Cb

Excitation of resonances in atoms with inner-shell vacancies has been under considerable theoretical and experimental study recently [1–5]. In addition to basic phenomena of intrinsic physical interest, there are two main reasons for these studies: the potential for novel practical applications in principle [1, 3], and the advent of high-intensity sources, such as the X-ray free-electron laser (XFEL) [6], required to create a high-energy-density (HED) [14] plasma containing the "hollow" atomic ions. In earlier theoretical investigations of K-shell resonances [1,3] we showed that the cross sections for resonant photo-excitations of  $K\alpha$ ,  $K\beta$ , etc. are orders of magnitude higher than the photoionization continua lying below the K-edge. The corresponding resonances or channels [3] become energetically accessible following K-shell ionization and Auger decays that open up multiple electronic vacancies in higher shells, particularly in high-Z atoms such as iron, platinum and gold [1, 9]. Following works have labelled these as "hidden" resonances [4] created in double-core-excited 'hollow' ions [5].

However, there are several problems in probing the dynamics of inner-shell resonant excitation. A monochromatic source is necessary to scan across the resonance energies. Sufficiently high intensities are necessary to create and achieve plasma conditions for deep electronic shell vacancies to exist. Extremely short pulse time-scales comparable to intrinsic atomic transition rates are required for *in situ* studies of resonant excitation. These criteria and problems have been addressed by recent XFEL studies, albeit for low Z atomic species where resonant rates are much smaller than the high Z atoms considered theoretically [1, 3]. Neon and aluminum ions were the focus of such experiments at the Stanford Linear Accelerator (SLAC) using the Linac Coherent Light Source (LCLS) XFEL [2, 5]. The peak intensities are extremely high, approximately  $10^{17}$  W cm<sup>-2</sup>. Experimental diagnosis centered on  $K\alpha$  resonance fluorescence (hereafter RFL): K-shell ionization followed by  $K\alpha$  emission creating a vacancy in the L-shell, following by resonance  $K \rightarrow L$  resonant excitation. Earlier theoretical calculations for transition probabilities and cross sections of several high

Z elements [7–9] were carried out for all ionization states possibly involved in  $K\alpha$  excitations, from H-like to F-like ions, and all resonances from  $K\alpha$  to  $K\eta$ , i.e.  $K \rightarrow L, M, N, O, P$  [1, 9]. In this *Letter* we establish a correspondence between the observed  $K\alpha$  resonances in Al ions [2] and the computed resonant absorption that drives  $K\alpha$  RFL, leading to an "enhancement" of the Auger effect (Fig.2, Ref. [1]).

The extremely high intensities needed to first create and then pump these resonances appear to make it impractical for any potential applications in the near future. While X-ray sources such as synchrotrons [10, 11], and now XFEL, are monochromatic and capable of high fluence that enables new experimentation, they are not readily available or suitable for technological or biomedical use. Whereas the task of creating deep inner-shell holes remains daunting in ordinary situations, it is worth asking what might be the *least* energetic requirement to pump RFL efficiently. In this report we also propose a schematic twin-beam monochromatic X-ray setup which might, in turn, enable applications such as localized X-ray deposition using high-Z radiosensitization in radiation therapy. Other effects related to Auger transitions, such as Rabi oscillations, and ultra-short femtosecond monochromatic X-ray pulses, are briefly discussed.

The LCLS-XFEL is sufficiently intense to create a solid-density plasma, where several ionization states of an element may exist with K-shell vacancies. When the FEL energy equals the  $K\alpha$  energy of an ion, RFL occurs and manifests itself as  $K\alpha$  emission which can be detected. The aluminium plasma created in the LCLS-XFEL experiment exhibited RFL for several ions at energies below the K-edge [2]. The resonance energies and strengths may be computed for all such ions, and all resonance transitions from the K-shell upwards leading up to K-edge [1]. However, including fine structure, there are a large number of  $K\alpha$  transitions that come into play: a total of 112 transitions are quantum mechanically allowed for all ions from H- to F-like [7, 12, 13]. Many of these overlap among adjacent ionization states. In order to facilitate a correspondence with  $K\alpha$  RFL measurements, we

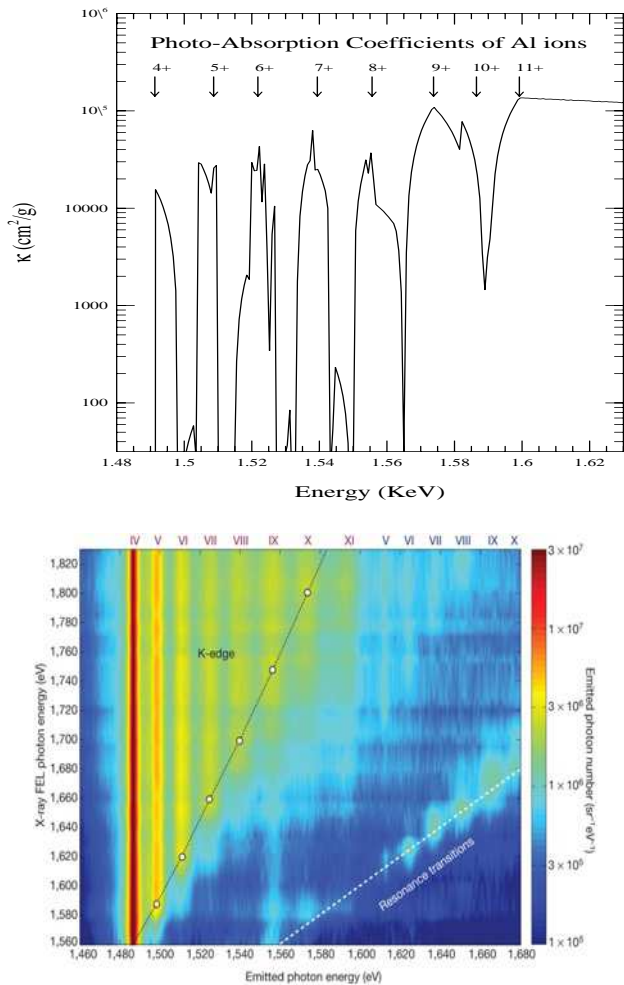


Figure 1: (color online). Top:  $K\alpha$  resonance fluorescence in aluminum plasma: Theoretically computed  $K\alpha$  absorption features in Al ions isoelectronic with fluorine to helium are shown (ionization states are labeled according to ion charge in the upper panel and roman numerals in the lower panel). All contributing  $K\alpha$  transition strengths are added together and shown in terms of X-ray attenuation coefficients  $\kappa$  (cm<sup>2</sup>/g) through the Al plasma (convolved over a gaussian FWHM of 10 eV). Bottom: Experimental measurements from the LCLS-XFEL [2] (reproduced with permission). The dashed line on the right shows the resonance transitions with increasing  $K\alpha$  emission intensity corresponding to the theoretical absorption complexes. The observed  $K\alpha$  features occur when the XFEL energy equals the emitted photon energy.

have computed only the  $K\alpha$  resonant absorption attenuation coefficients (cm<sup>2</sup>/g) taking account of overlapping profiles. The resulting  $K\alpha$  absorption that drives RFL pumping is shown in Fig. 1, and compared with the experimental results.

The cross sections used to compute the resonance structures in Fig. 1 were convolved with a small gaussian beam width of 10 eV FWHM. The calculations are carried out using the Breit-Pauli version of the atomic structure

and R-matrix codes [13]. Evidently, the  $K\alpha$  absorption resonance complexes for each ion can be associated with the  $K\alpha$  emission seen experimentally (lower panel). The rising trend in relative intensities, measured as "Emitted photon number (sr<sup>-1</sup>eV<sup>-1</sup>)" [2], is also evident in the theoretical  $K\alpha$  resonance strengths for successively higher ionization states of Al (upper panel). The experimental data in the lower panel exhibit overlaps and different total intensities of the various  $K\alpha$  complexes. That is also seen qualitatively in the top panel with aggregate  $K\alpha$  resonance strengths for each ion. A more quantitative description of averaged energies and  $K\alpha$  resonance strengths is given in Table 1 for H- to F-like ionization states for aluminum. The number of transitions, and relative positions and  $K\alpha$  strengths, can be discerned readily from the fine structure averaged energies and cross sections (megabarns) derived from resonance oscillator strengths.

Table 1 also presents the positions and  $K\alpha$  resonance strengths for possible experimental detection thereof for titanium. Fig. 2 shows the  $K\alpha$  resonance complexes for titanium. A similar structure as for Al is evident. The possibility of experimental observations of Ti  $K\alpha$  resonances at the LCLS-XFEL suggest itself, at the averaged energies and strengths given in Table 1 for each Ti ion. While for Al ions  $K\alpha$  resonance fluorescence occurs in the 1.48-1.88 keV range, the corresponding range for Ti  $K\alpha$  resonances is 4.5-5 keV. The LCLS-XFEL is capable of energies up to about 8 keV in the fundamental mode, well above the Ti  $K\alpha$  energies (or even the Fe  $K\alpha$  energies <6.9 keV [1]). A more complete account of the atomic calculations and models of related processes will be given elsewhere. Here we note that in addition to the primary physical process of an L-shell vacancy pumped by K-shell photo-excitation, there are several, often competing, processes that need to be accounted for. These include Auger decays and radiative cascades from outer shells, electron impact ionization dependent on plasma density, and resonance broadening and overlap.

The fact that a direct correspondence between  $K\alpha$  resonance complexes and the  $K\alpha$  emission in a high-density and high-intensity environment created in an XFEL can be established, reveals not only the nature of these resonances but also their excitation mechanism. However, highly intense monochromatic XFEL beams or synchrotron sources producing a HED plasma are impractical for most common applications and environments unable to withstand such intensities. Other monochromatic X-ray sources are being developed using peta-watt lasers for plasma imaging and  $K\alpha$  radiography (e.g. [15–17]). These are also very intense sources, with  $K\alpha$  conversion efficiencies of  $\sim 10^{-4}$  in the range of laser intensities of  $10^{18-20}$  W/cm<sup>2</sup>. On the other hand, a low intensity monochromatic X-ray source may not contain sufficient fluence to be effective in creating and pumping  $K\alpha$  RFL for useful purposes. In particular, monochromatic X-ray biomedical imaging and therapeutics would need far less intense fluxes. One may therefore ask the

Table I: Averaged  $K\alpha$  Resonant Energies and Cross Sections for Al and Ti Ions

Ion Core	Transition Array	# of Transitions	Al		Ti	
			$\langle E(K\alpha) \rangle$ (keV)	$\langle \sigma_{res}(K\alpha) \rangle$ (Mb)	$\langle E(K\alpha) \rangle$ (keV)	$\langle \sigma_{res}(K\alpha) \rangle$ (Mb)
F-like	$1s^2 2s^2 2p^5 - 1s 2s^2 2p^6$	2	1.491	1.40	4.541	1.73
O-like	$1s^2 2s^2 2p^4 - 1s 2s^2 2p^5$	14	1.509	7.05	4.575	8.63
N-like	$1s^2 2s^2 2p^3 - 1s 2s^2 2p^4$	35	1.522	11.2	4.604	13.3
C-like	$1s^2 2s^2 2p^2 - 1s 2s^2 2p^3$	35	1.539	15.4	4.639	17.9
B-like	$1s^2 2s^2 2p^1 - 1s 2s^2 2p^2$	14	1.556	8.20	4.671	9.22
Be-like	$1s^2 2s^2 - 1s 2s^2 2p$	2	1.574	4.93	4.708	5.47
Li-like	$1s^2 2s - 1s 2s 2p$	6	1.587	5.70	4.732	6.01
He-like	$1s^2 - 1s 2p$	2	1.599	6.11	4.755	6.24
H-like	$1s - 2p$	2	1.789	3.33	4.975	3.28

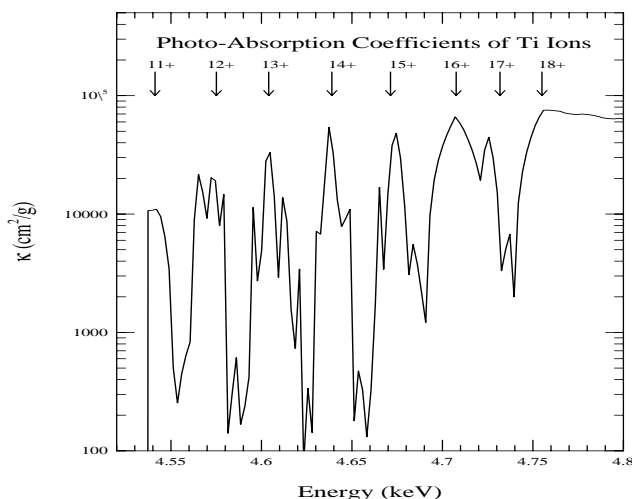


Figure 2: Titanium  $K\alpha$  resonance complexes, as in Fig. 1 (top panel for aluminum ions). For clarity, the H-like  $Ti^{19+}$   $K\alpha$  resonances are omitted since they lie significantly above the He-like  $Ti^{18+}$  complex (also in Fig. 1 for Al ions). The Ti  $K\alpha$  resonance fluorescence has not yet been observed, but the energies are in the accessible range of beam energies at the LCLS-XFEL. The XFEL energies may be scanned across the calculated average  $K\alpha$  energies for each ion given in Table 1.

question (albeit theoretically): what is the minimum intensity of an X-ray beam, or a combination of x-ray beams, that can be employed in principle to excite or pump  $K\alpha$  RFL? The femto-second, or shorter, timescales are commensurate with atomic transition rates (Einstein A and B-coefficients), and hence Auger decay radiative cascade rates. A monochromatic X-ray beam could produce enough  $K\alpha$  photon flux to pump K-shell electrons, in competition with downward decay rates, provided L-shell vacancies exist *a priori*.

One possibility to minimize the incident flux required

for  $K\alpha$  RFL is a twin-beam monochromatic X-ray device [25], schematically illustrated in Fig. 3. The two beams are tuned to the K-edge and the  $K\alpha$  resonance energies respectively. K-shell ionizations induced by the first beam would lead to electron vacancies in the L and higher shells via Auger decays. The second beam would pump the RFL mechanism, as well as cause secondary ionizations from the emitted photon and electron ejections. The excitation/ionization processes are coupled, and dependent on photon fluences of the two beams. Ultrafast monochromatic X-ray sources, such as the ones based on femtosecond PW lasers, would be suitable for the twin-beam configuration. A generalization of the proposed embodiment in Fig. 3, utilizing multiple monochromatic X-ray beams, may also be implemented. Such an extended system could target higher than  $K\alpha$  resonance complexes, as discussed in [1].

Potential applications of monochromatic X-ray systems have been proposed in biomedical spectroscopy for imaging and therapy. For example, synchrotron sources tuned to the K-edge have been employed to explore the breakdown of high-Z compounds of platinum or gold in nanoentities, to be delivered to tumors and kill cancer cells upon irradiation [10, 11, 18, 19]. Recent theoretical studies have shown that relatively low energy X-rays in the  $E < 100$  keV range should be far more effective than the conventional high energy X-rays in the MeV range generated by linear accelerators (LINACs) used in radiation therapy (e.g. [20–23]). Monochromatic X-ray systems, if available, might be ideal. The radiation dose generally tolerated in radiation treatment is approximately 1 Gray (Gy) per minute (usually not to exceed a few tens of Gys). Given that  $1 \text{ Gy} = 1 \text{ J/Kg}$ , PW lasers, or combination thereof, can generate this amount of X-ray flux for radiation treatment (a radiation dose of 1 Gy is roughly equivalent to approximately  $10^{10}$  photons of 80 keV energy directed at body tissue with area  $1 \text{ cm}^2$ ).

A serious problem with  $E < 100$  keV radiation is the factor of 2 or 3 larger attenuation coefficients inside the body than the high energy MeV X-rays, rendering the former unsuitable for treatment of deeply located tumors

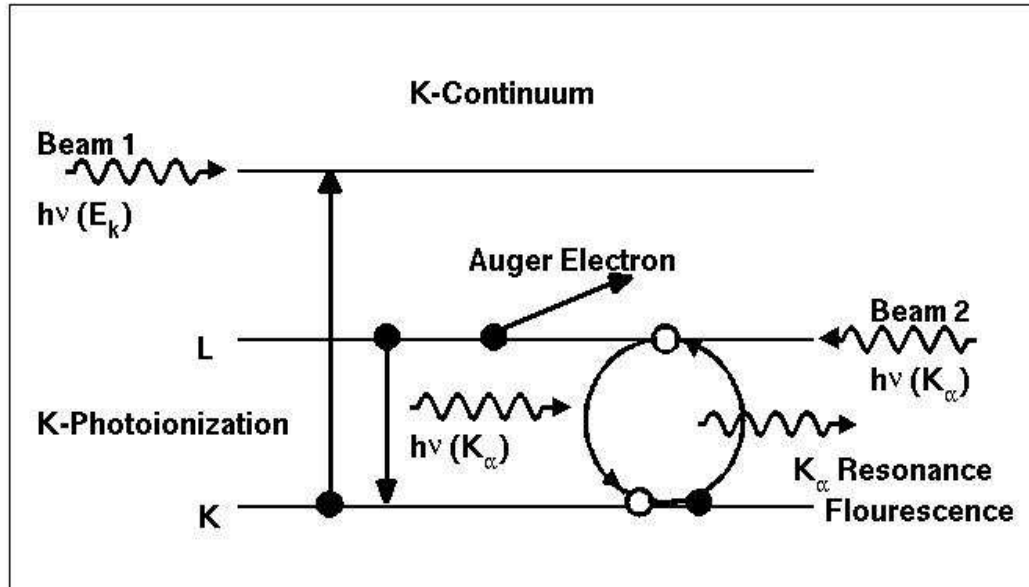


Figure 3: Schematic diagram of a twin-beam monochromatic X-ray system. K-shell ionization by Beam 1 (on the left) triggers the Auger decays, and  $K\alpha$  resonance fluorescence is pumped and driven by Beam 2 (on the right).

inside the body; that is the *raison d'être* for employing high energy LINACs [23]. But the cross sections for photoionization, that trigger Auger decays and ejected electron yields, decrease as  $\sigma_{PI} \sim E^{-3}$ , whereas Compton scattering cross sections increase with energy until they exceed photoelectric absorption by orders of magnitude well below the MeV range [24]. Therefore high energy photons are preferentially scattered inside the body, rather than result in Auger electron yields that might destroy cancer cells sensitized with high-Z nanomaterials. Monte Carlo numerical simulations have shown that radiosensitization factors of Pt or Au with low energy X-rays with mean energies  $E \sim 100$  keV are an order of magnitude higher, and therefore could more than compensate for their reduced attenuation and be more effective than high energy MeV photons [23]. Also, the use of broadband radiation sources, such as the LINACs, is also wasteful since bremsstrahlung output spectrum lacks specificity in energy and penetration depth. Therefore, tunable monochromatic X-ray sources would be preferable. In addition, the efficacy of high-Z contrast agents could be greatly enhanced if the  $K\alpha$  RFL mechanism described in this *Letter* can be implemented in practice. Driving the  $K\alpha$  Auger cycle with monochromatic X-ray system(s) would result in increased local energy deposition than by K-shell ionization alone.

A numerical collisional-radiative model may be constructed to simulate the physical processes illustrated in Fig. 3. The model would employ atomic rates for ex-

citation, ionization, photon fluences  $\Phi_1, \Phi_2$  in beams 1 and 2 respectively, K and L level populations, cascade coefficients from upper shells, etc. For instance, the L-shell population for each ion is governed by direct photoionizations by the two beams with  $\Phi_1$  and  $\Phi_2$ , collisional ionizations by electrons in the plasma at local density and temperature, cascades from outer shells, resonant excitation from the K-shell as well as stimulated emission  $L \rightarrow K$  that constitutes the Auger cycle. Also, given the photon fluences in the two beams, we may obtain an estimate of induced Rabi oscillations at frequency  $\omega_R = \mu_{KL}E/\hbar$ , where  $\mu_{KL}$  is the dipole moment related to the A-coefficient for a given  $K \rightarrow L$  transition, and  $E$  is the electric field amplitude corresponding to the irradiance (time-averaged power per unit area)  $I = \frac{1}{2}c\epsilon_0 E^2$  in beam 2 with fluence  $\Phi_2$ . Though complex, such as model is computationally feasible. However, the primary requirement is the calculation of the cross sections, transition probabilities, and rates for all contributing processes mentioned above. Work is in progress along these directions.

We would like to thank Sara Lim and Michael Dance for contributions. This work was partially supported by grants from the U.S. Department of Energy, National Nuclear Stewardship Alliance program (DE-FG52-09NA29580), and the National Science Foundation (AST-0907763).

\* nahar.1@osu.edu, † pradhan.1@osu.edu

- 
- [1] A. K. Pradhan, S. N. Nahar, M. Montenegro, Y. Yu, H. L. Zhang, C. Sur, M. Mroziak, and R. M. Pitzer, *J. Phys. Chem. A* **113**, 12356 (2009).
- [2] S. M. Vinko *et al.*, *Nature* **482**, 59 (2012).
- [3] M. Montenegro, S. N. Nahar, A. K. Pradhan, K. Huang, and Y. Yu, *J. Phys. Chem. A* **113**, 12364 (2009).
- [4] E. P. Kanter *et al.*, *Phys. Rev. Lett.* **107**, 233001 (2011).
- [5] N. Rohringer *et al.*, *Nature* **26**, 488 (2012).
- [6] L. Young *et al.*, *Nature* **466**, 56 (2010).
- [7] S. N. Nahar, A. K. Pradhan, and C. Sur, *J. Quant. Spectrosc. Radiat. Transfer* **109**, 1951 (2008).
- [8] C. Sur, S. N. Nahar, and A. K. Pradhan, *Phys. Rev. A* **77**, 052502, (2008).
- [9] S. N. Nahar, A. K. Pradhan, and S. Lim, *Can. J. Phys.* **89**, 483 (2011).
- [10] H. Elleaume, A. M. Charvet, P. Berkevens *et al.*, *Nucl. Inst. Meth. Phys. Res. A* **428**, 513 (1999).
- [11] K. Kobayashi, N. Usami, E. Porcel, S. Lacombe, C. Le Sech, *Mutation Research* **704**, 123 (2010).
- [12] S. N. Nahar, W. Eissner, G.-X. Chen and A. K. Pradhan, *Astron. Astrophys.* **408**, 789 (2003); W. Eissner, M. Jones & H. Nussbaumer, *Comput. Phys. Commun.* **8**, 270 (1974).
- [13] A. K. Pradhan and S. N. Nahar, *Atomic Astrophysics and Spectroscopy*, Cambridge University Press (2011).
- [14] R. P. Drake, *High Energy Density Physics*, Springer (2006).
- [15] H. S. Park *et al.*, *Phys. Plasmas* **13**, 056309 (2009).
- [16] K. Akli *et al.*, *Rev. Sci. Instrum.* **82**, 123503 (2011).
- [17] K. Akli *et al.*, *Phys. Plasmas* **18**, 112702 (2011).
- [18] W. Yang *et al.*, *J. Neurooncology* **101**, 379390 (2010).
- [19] E. Procel *et al.*, *Nanotechnology* **21**, 1 (2010).
- [20] M. K. K. Leung *et al.*, *Med. Phys.* **38**(2), 624 (2011).
- [21] R. I. Berbeco, W. Ngwa and G. M. Makrigiorgos, *Int. J. Rad. Oncol. Biol. Phys.* **81**(1), 270276 (2011).
- [22] S. Jain *et al.*, *Int. J. Rad. Oncol. Biol. Phys.* **79**(2), 531 (2011).
- [23] S. Lim *et al.* (submitted).
- [24] National Institute for Standards and Technology (NIST), X-ray cross section database XCOM at <http://www.nist.gov/pml/data/xcom/index.cfm>
- [25] International Patent Cooperation Treaty (PCT) Application (pending) WO 2012/054471 A1, *Monochromatic X-ray Devices and Methods of Use*, The Ohio State University and the Thomas Jefferson University (Anil K. Pradhan and Yan Yu).